Multi-user detection for the ARGOS satellite system

Benoît Escrig, Fares Fares, Marie-Laure Boucheret, Thibaud Calmettes, Hervé Guillon

HAL Id: hal-01123503

https://hal.science/hal-01123503

Submitted on 5 Mar 2015

Multi-User Detection for the ARGOS Satellite System

Benoît Escrig[1*] Fares Fares[1] Marie-Laure Boucheret[1] Thibaud Calmettes[2] and Hervé Guillon[3]

[1] *Signal and Communications Team, IRIT Laboratory, Toulouse, France*
[2] *Thalès Alenia Space (TAS), Toulouse, France*
[3] *Centre National d'Etudes Spatiales (CNES), Toulouse, France*

SUMMARY

In this paper, we evaluate several Multi-User Detection (MUD) architectures for the reception of asynchronous beacon signals in the ARGOS satellite system. The case of synchronous signals is studied first. Though impractical, this case provides useful guidance on the second part of the study, i.e., the design of MUD receivers for asynchronous users. This paper focuses more particularly on Successive Interference Cancellation (SIC) receivers since they have been shown to achieve a good performance complexity trade-off. Several E_b/N_0 degradation curves are obtained as a function of channel parameters. With these curves, a performance analysis is presented in order to determine in which conditions it is possible to successfully decode none, one, or more beacon signals. We show that SIC receivers can improve the percentage of served beacons from 50% to more than 67% for a population of 37,600 beacons. Copyright © 0000 John Wiley & Sons, Ltd.

KEY WORDS: ARGOS System, Multi-User Detection, Successive Interference Cancellation

1. INTRODUCTION

The ARGOS system is a satellite system dedicated to the study of the environment [1, 2]. ARGOS beacons transmit their data periodically to low polar orbit satellites that receive, decode, and then forward the data to ground processing stations [3]. One of the major issues of the ARGOS system concerns the service rate, i.e., the percentage of visible beacons that are successfully processed

---

*Correspondence to: ENSEEIHT, Rue Camichel, 31071 Toulouse, France, E-mail: escrig@enseeiht.fr

by an ARGOS satellite[†]. The service rate is decreasing with the increasing number of beacons. It is now 68% for a population of 21,000 beacons but it will fall under 50% when the population will reach 37,600. This is because the Multiple Access Interference (MAI) at the ARGOS satellite receivers is increasing with the number of deployed beacons and the satellite receivers have not been designed to take into account this kind of interference. The origin of the MAI is twofold. First, the relative motion between the beacons and the satellites induces large Doppler shifts on the transmitted frequencies, so the emitted signals overlap in frequency. This happens despite the fact that each beacon has its own carrier frequency. Second, the signals overlap in time since there is no time synchronization between the users. Increasing the system bandwidth or designing spectrally efficient waveforms only provide short term solutions since these techniques do not tackle the main problem, i.e., the suppression of the MAI. In this paper, we address this issue by designing Multi-User Detection (MUD) receivers. MUD techniques have been widely used in the context of Code Division Multiple Access (CDMA) systems [4, 5]. Several CDMA-based satellite systems using MUD receivers have proposed [6, 7]. We review these techniques and evaluate their suitability for the ARGOS system. Besides, MUD receivers have been proposed for satellite systems such as the automatic identification system (AIS). The approaches are based on a multi-beam receiver [8, 9]. In this paper, we limit ourselves to the study of two beacon signals. Our goal is to determine the conditions in which two signals are successfully decoded when two signals are received at the satellite. This is a first step toward the successful decoding of all the colliding signals.

We first design MUD receivers in the synchronous case, i.e., when the beacon signals are all received at the same time at the satellite. Although this case is unrealistic, it provides useful guidance on the design of MUD techniques in the asynchronous case. The receivers are evaluated in terms of Bit Error Rate (BER) as a function of several system parameters: the relative frequency shift and the signal to interference ratio between the two received signals, and the E_b/N_0 ratio, where E_b is the average energy received per bit and N_0 is half the noise variance of the AWGN (Additive White Gaussian Noise) channel. Note that the E_b/N_0 ratio is similar to a Signal to Noise Ratio (SNR) per bit. MUD receivers for the asynchronous case are then designed and evaluated. Thereafter, a performance analysis is performed so that it is now possible to determine the range of values over which none, one, or more user signals can be successfully decoded. When two users are received simultaneously by the satellite and the satellite is equipped with a receiver that can process two users, we show that our approach is able to process 98% of the cases. In this way, the service

---

[†]Note that only 6% of the total number of beacons are visible from an ARGOS satellite.

rate can reach 83% for a population of 37,600 beacons when the signals parameters are perfectly estimated, and 67% when imperfect parameter estimation is considered.

The rest of the paper is organized as follows. In Section 2, we present the system model. The MUD techniques for the synchronous case are presented and evaluated in Section 3. A similar approach is undertaken for the asynchronous case in Section 4. The performance analysis is performed in Section 5 and we conclude in the last section.

2. SYSTEM DESCRIPTION

This section describes both the beacon signals and the signals received by the satellites. Channel impairments and design constraints are also addressed. In this paper, we concentrate on standard beacons. More recent beacons, based on new frame formats, have been defined since then, but they are dedicated to specific applications.

2.1. Beacon signals

Beacon signals comprise a non-modulated part and a modulated part. In the non-modulated part, only the carrier signal is present. This part lasts 160 ms $\pm\,2.5$ ms. Data bits and control bits are modulating the amplitude of the carrier signal in the modulated part. The data rate is $R = 400$ bit/s with a tolerance of 1.25%. Beacon signals last from 360 ms to 920 ms according to the frame format. A Pulse Code Modulation/Phase Modulation (PCM/PM) modulation technique [10] is implemented with a modulation index $m = 1.1$ in radians[‡]. Each beacon k is transmitting a signal $s_k(t)$

$$s_k(t) = \sqrt{2P_t} \cos[2\pi f_k t + \theta_k + m d_k(t)] \tag{1}$$

where P_t denotes the emitted power by the beacon, f_k and θ_k denote the carrier frequency and the phase of the emitted signal, respectively. The information stream of user (beacon) k, denoted $d_k(t)$, is given by

$$d_k(t) = \sum_{n=0}^{M-1} b_k(n) h(t - nT)$$

where M in the number of symbols per user message, $b_k(n) \in \{-1, +1\}$ denotes the nth symbol emitted at time nT, T being the symbol period ($T = 1/R$), and $h(t)$ is the unit energy bi-phase

---

[‡]Residual carrier modulations such as the PCM/PM modulation scheme are usually used to assist the receiver in demodulating the signal.

signature waveform with a value of $1/\sqrt{T}$ over the interval $[0, T/2]$ and a value of $-1/\sqrt{T}$ over the interval $[T/2, T]$. The carrier frequency f_k is in the interval 401.61 MHz $\leq f_k \leq 401.69$ MHz and the repetition period T_r, i.e., the time between two consecutive transmissions of the same ARGOS message, is in the interval 60 s $\leq T_r \leq 200$ s. Since $d_k(t)(n) \in \pm 1$, (1) can be rewritten as

$$s_k(t) = \mathrm{Re}\{\sqrt{2P_t}[\cos(m) + j sin(m)d_k(t)]\exp[j2\pi f_k t + \theta_k]\} \tag{2}$$

2.2. Channel impairments

Satellite channels are typically modeled as AWGN channels but transmissions are also affected by frequency drifts. These drifts are due to oscillator instabilities (1 kHz), Doppler shifts (9 kHz maximum), and Doppler drifts (85 Hz/s maximum). As a result, beacon signals are overlapping at the receiver side, both in frequency and in time, since there is no way to synchronize the beacon transmissions. Moreover, the maximum free-space-loss difference between two received beacon signals may be as high as 10.5 dB and the time difference between two simultaneously transmitted signals may be as high as 6.5 ms. Note that path losses and shadowing effects are not considered here since link budget issues are assumed to be solved at the first stage of the receiver.

2.3. Received Signals

Let $r(t)$ be the low-pass signal associated with the band-pass signal received at the satellite. Assuming that K users have been simultaneously transmitted, the signal emitted by user k, $s_k(t)$, has been defined in (1) for $1 \leq k \leq K$. So, we have that

$$r(t) = \sum_{k=1}^{K} r_k(t - \tau_k) + \eta(t) \tag{3}$$

where $\eta(t)$ is a circularly symmetric complex Gaussian noise with variance $\sigma^2 = 2N_0$. Signals $r_k(t - \tau_k)$ are low-pass signals, where τ_k is the time delay of user k. They are obtained using (2)

$$r_k(t) = A_k[\cos(m) + j\sin(m)\sum_{n=0}^{M-1} b_k(n)h(t - nT)] \times \exp[j(2\pi\Delta f_k t + \theta_k)]$$

where A_k is the amplitude received from user k, $k \in [1, K]$ and Δf_k is the frequency shift of user k given by $\Delta f_k = f_k^{(r)} - f_l^{(r)}$ where $f_k^{(r)}$ denotes the received carrier frequency from user k, taking into account the Doppler effect and $f_l^{(r)}$ denotes the received carrier frequency for a specific user of interest, denoted l, $l \in [1, K]$. The parameters A_k, Δf_k, τ_k, and θ_k are assumed to have

known constant values over the duration of a data frame. The estimation of the signal parameters is addressed at the end of the paper. Frequency and phase jitters are not considered in this paper. We also assume that the time delays are sorted in ascending order, i.e.,

$$0 = \tau_1 \leq \tau_2 \leq \ldots \leq \tau_K \tag{4}$$

Only the modulated part is considered in this paper. The non-modulated part is used for synchronization purposes.

3. MUD RECEIVERS FOR SYNCHRONOUS ARGOS USERS

MUD receivers for the synchronous case are presented in this section [11]. The delays in (3) are all zeros, i.e., $\tau_1 = \tau_2 = \ldots = \tau_K = 0$. We begin by expressing the output of the matched filter and then give the matrix representation of the problem. With these relations at hand, we propose several MUD receivers.

3.1. Matched Filter Output and Matrix Representation

We consider the transmission of K synchronous users in an AWGN channel. To decode the message of user l, the band-pass received signal $r(t)$ is first converted to a low-pass signal and then passed through a matched filter $h^*(-t)$. Let $y_l(u)$ be the output of the matched filter for the uth symbol transmitted at time uT, $0 \leq u \leq M - 1$, by user l

$$y_l(u) = \int_{uT}^{(u+1)T} r(t) \exp[-j(2\pi\Delta f_l t + \theta_l)]h^*(t - uT)dt \tag{5}$$

where the superscript * denotes the complex conjugate. Replacing $r(t)$ in (5) by its expression in (3), we have that

$$y_l(u) = \sum_{k=1}^{K} A_k \cos(m)\rho'_{(l,k)}(u) + j\sum_{k=1}^{K}\sum_{n=0}^{M-1} A_k \sin(m)b_k(u)\rho_{(l,k)}(u,n) + \eta_l(u) \tag{6}$$

where $\eta_l(u)$ denotes the noise at the output of the matched filter of user l at time uT. The index u is used for user l and the index n is used for other users k. The coefficient $\rho'_{l,k}(u)$ denotes the

correlation due to the residual carriers of users l and k

$$\rho'_{l,k}(u) = \int_{uT}^{(u+1)T} \exp\{j[2\pi(\Delta f_k - \Delta f_l)t + \theta_k - \theta_l]\}h^*(t - uT)dt$$

The coefficient $\rho_{l,k}(u,n)$ denotes the correlation from the data symbols at instants uT and nT between user l and the interfering user k

$$\rho_{l,k}(u,n) = \int_{uT}^{(u+1)T} \exp\{j[2\pi(\Delta f_k - \Delta f_l)t + \theta_k - \theta_l]\}h(t - nT)h^*(t - uT)dt$$

Note that these coefficients are time-varying whereas correlation coefficients in CDMA systems are not. The design of shaping filters that minimize the correlation coefficients will be addressed in future work. The complex Gaussian noise component $\eta_l(u)$ at the output of the matched filter is given by

$$\eta_l(u) = \int_{uT}^{(u+1)T} \exp[-j(2\pi\Delta f_l t + \theta_l)]h^*(t - uT)dt$$

Since $h(t)$ is zero outside the interval $[0, T]$, the coefficients $\rho_{l,k}(u,n)$ are zeros for $n \neq u$. So from (6), we have that

$$y_l(u) = \sum_{k=1}^{K} A_k[\cos(m)\rho'_{(l,k)}(u) + j\sin(m)b_k(u)\rho_{(l,k)}(u,n)] + \eta_l(u) \tag{7}$$

The correlation coefficients can be expressed as

$$\rho'_{(l,k)}(u) = \zeta_{l,k}(0, T/2, u) - \zeta_{l,k}(T/2, T, u) \text{ and } \rho_{(l,k)}(u,n) = \zeta_{l,k}(0, T, u) \tag{8}$$

where

$$\zeta_{l,k}(a, b, u) = (b - a)\text{sinc}[(\Delta f_k - \Delta f_l)(b - a)]f_{l,k}(a, b, u) \tag{9}$$

and $f_{l,k}(a, b, u) = \exp\{j[\pi(\Delta f_k - \Delta f_l)(a + b + 2uT) + \theta_k - \theta_l\}$. The two sets of coefficients have the Hermitian property, i.e., $\rho_{(l,k)}(u,n) = \rho^*_{(k,l)}(u,n)$ and $\rho'_{(l,k)}(u) = \rho'^*_{(k,l)}(u)$. These coefficients are time dependent coefficients. They also depend on both the symbol period and the frequency differences $|\Delta f_k - \Delta f_l|$ between two user signals. Note that these frequency differences are not adjustable. We now express $y_l(u)$ in a matrix form by rewriting (7)

$$\mathbf{y}(u) = \mathbf{R}'(u)\cos(m)\mathbf{A}\mathbf{1}_{K\times 1} + j\mathbf{R}(u, u)\sin(m)\mathbf{A}\mathbf{b}(u) + \mathbf{n}(u) \tag{10}$$

where $\mathbf{R}^{'}(u) \in \mathbb{C}^{K \times K}$ is the residual carrier cross correlation matrix with general term $\rho^{'}_{(l,k)}(u)$, $\mathbf{A}$ is the $K \times K$ diagonal matrix with general term A_l, $\mathbf{R}(u,u) \in \mathbb{C}^{K \times K}$ is the cross correlation matrix with general term $\rho_{(l,k)}(u,u)$, $\mathbf{1}_{K \times 1}$ is a unity vector $\mathbf{1}_{K \times 1} = [1 \ldots 1]^T$, and the superscript ^{T} denotes the transpose operator. We define also the following column vectors of length K: $\mathbf{y}(u) = [y_1(u)y_2(u) \ldots y_K(u)]^T$, $\mathbf{b}(u) = [b_1(u)b_2(u) \ldots b_K(u)]^T$, and $\mathbf{n}(u) = [\eta_1(u)\eta_2(u) \ldots \eta_K(u)]^T$. Note that the vector $\mathbf{n}(u)$ is a $1 \times K$ vector with zero mean and covariance matrix $\sigma^2 \mathbf{R}(u,u)$.

3.2. MUD Receivers for Synchronous Beacon Transmissions

Several MUD receivers are presented: the Maximum Likelihood (ML) detector, the conventional receiver, the decorrelator detector, and the Minimum Mean Square Error (MMSE) receiver. Interference Cancellation (IC) techniques are also investigated: the Successive IC (SIC) receiver and the Parallel IC (PIC) receiver [12–15].

3.2.1. Maximum Likelihood Detector The ML detector performs an exhaustive search on all the possible sequences of the vector $\mathbf{b}(u)$, for $0 \leq u \leq M - 1$

$$\hat{\mathbf{b}}(u) = \underset{\mathbf{b}(u) \in \mathbf{B}(u)}{\operatorname{argmax}} \{P[r(t), uT \leq t \leq (u+1)T | \mathbf{b}(u)]\} = \underset{\mathbf{b}(u) \in \mathbf{B}(u)}{\operatorname{argmax}} F[\mathbf{b}(u)]$$

where $\mathbf{B}(u)$ is the set of all the possible sequences of the vector $\mathbf{b}(u)$ and

$$F[\mathbf{b}(u)] = \frac{1}{\sqrt{2\pi\sigma^2}} \exp\left[\int_{uT}^{(u+1)T} -\frac{1}{2\sigma^2}|r(t) - s_{\mathbf{b}(u)}(t)|^2 dt\right] \tag{11}$$

where $s_{\mathbf{b}(u)}(t)$ is defined as

$$s_{\mathbf{b}(u)}(t) = \sum_{k=1}^{K} A_k[\cos(m) + j\sin(m)b_k(u)h(t - uT)] \exp[j(2\pi\Delta f_k t + \theta_k)] \tag{12}$$

We rewrite (11) and suppress the terms that do not depend on $\mathbf{b}(u)$. So, we have that

$$F[\mathbf{b}(u)] = 2\operatorname{Re}\left[\int_{uT}^{(u+1)T} r(t)s_{\mathbf{b}(u)}^*(t)dt\right] - \int_{uT}^{(u+1)T} s_{\mathbf{b}(u)}(t)s_{\mathbf{b}(u)}^*(t)dt \tag{13}$$

Using (12) and the hermitian property, (13) can be rewritten as

$$
\begin{aligned}
F[\mathbf{b}(u)] \quad = \quad & 2\,\mathrm{Im}\left[\mathbf{b}^T(u)\sin(m)\mathbf{A}y(u)\right] - \mathbf{b}^T(u)\sin^2(m)\mathbf{AR}(u,u)\mathbf{Ab}(u) \\
+ \quad & 2\,\mathrm{Im}\left[\mathbf{1}_{K\times 1}^T\cos(m)\sin(m)\mathbf{AR}^{'}(u)\mathbf{Ab}(u)\right]
\end{aligned}
$$

Hence, the optimal detector consists of K matched filters followed by a detector based on an exhaustive search of the best symbol sequence in a set of 2^K possible sequences. This detector, though optimal in terms of error probability, is known to have a computational load that grows exponentially with the number of users. So, alternative solutions should be developed in order to take into account this issue.

3.2.2. Conventional Receiver The conventional receiver consists of K mono-user detectors in parallel. The detector is directly fed with the output of the matched filter, so we have that

$$
\hat{b}_l(u) = \underset{b_l(u)\in\{-1,+1\}}{\mathrm{argmax}} \{\mathrm{P}[y_l(u)|b_l(u)]\} \tag{14}
$$

Here, the MAI is processed as an additive noise. So the detector becomes inefficient when a low power signal is received in the presence of a stronger interfering signal. This basic receiver can be improved by exploiting the structure of the correlation coefficients.

3.2.3. Decorrelator From (10), we note that the MAI appears in $y_l(u)$ as soon as the matrix $\mathbf{R}^{'}(u)$ is not diagonal. A first attempt to remove the MAI consists in performing a decorrelating operation on $\mathbf{y}(u)$, i.e., by computing $\mathbf{R}^{-1}(u,u)\mathbf{y}(u)$ [5]. From (10), we note also that the remaining interference is mostly caused by carrier residuals, not by symbols from other users. Note however that the noise part is amplified when $\mathbf{R}^{-1}(u,u)$ increases. This increase in the noise floor degrades the performance of the receiver. Note that the decorrelator performs poorly in the low SNR region.

3.2.4. MMSE receiver The decorrelator approach focusses on the minimization of the MAI. Instead, the MMSE receiver aims at minimizing the distance between the output of the MMSE receiver and the transmitted symbols [5]. This is achieved by computing the matrix $\mathbf{M}(u)$ that minimizes the expectation $\mathrm{E}[|\mathbf{b}(u) - \mathbf{M}(u)\mathbf{y}(u)|^2]$. So, we have that $\mathbf{M}(u) = [\mathbf{R}(u,u) + \sigma^2\mathbf{A}^{-2}]^{-1}$. Note that the MMSE method resembles the decorrelator method as the noise level vanishes and $\mathbf{M}(u)$ approaches $\mathbf{R}^{-1}(u,u)$.

3.2.5. Successive Interference Cancellation (SIC) Receiver The three previous MUD receivers perform poorly when the signal of interest is corrupted by interfering signals with higher power. This has motivated the design of IC-based receivers such as the SIC receiver [12–16]. We start the description this receiver by rewriting (3)

$$r(t) = \sum_{k=1}^{K} r_{(k)}(t) + \eta(t)$$

where $r_{(k)}(t)$ is the received signal with the kth largest power with amplitude $A_{(k)}$, frequency shift $\Delta f_{(k)}$, and carrier phase $\theta_{(k)}$. The signal $r(t)$ is first fed into a conventional receiver, that demodulates the signal with the largest power. The symbols $\hat{b}_{(1)}(u)$ for $u \in [0, M-1]$ are estimated using (14). Then, an estimated signal $\hat{r}_{(1)}(t)$ is obtained

$$\hat{r}_{(1)}(t) = A_{(1)} \left[cos(m) + j \sum_{u=0}^{M-1} sin(m)\hat{b}_{(1)}(u)h(t - nT) \right] \exp[j(2\pi\Delta f_{(1)}t + \theta_{(1)})]$$

This copy is subtracted from the received signal $r(t)$. The resulting signal $r(t) - \hat{r}_{(1)}(t)$ is fed into a second conventional receiver to demodulate the signal with the second largest power. These steps are repeated until a threshold $K_{\max}$ has been reached. In this paper, we limit ourselves to the case of two decoded users, i.e., $K_{\max} = 2$. Note that error propagation can occur when one user is not decoded successfully and this becomes even more evident when the number of concurrent beacons is higher than two. The BER performance of SIC receivers is improved when conventional receivers are replaced by MMSE receivers.

3.2.6. Parallel Interference Cancellation (PIC) Receiver The PIC receiver resembles the SIC receiver since is based on the same IC approach. The PIC receiver subtracts, at each stage, the estimated interference from all the users, in order to demodulate the user of interest. The interference is estimated by decoding the symbols from all the users, and by regenerating and summing the corresponding signals. Thus, better interference subtraction is performed. To decode the user of interest l, the input of the conventional receiver is

$$r(t) - \sum_{k=1, k\neq l}^{K_{\max}} \hat{r}_{(k)}(t)$$

where $\hat{r}_{(k)}(t)$ is an estimate of the signal $r_{(k)}(t)$. Conventional receivers may also be replaced by MMSE receivers to improve the BER performance of PIC receivers (MMSE-PIC receivers).

3.3. Simulations Results

In this section, we compare the BER performance of several MUD receivers in the synchronous case. We assume the reception of $K = 2$ users separated by a frequency shift Δf. Up to now, there is no multi-user receivers. Choosing $K = 2$ is the first step in the design of K multi-user receivers. Note that changing a single user receiver into a 2-user receiver increases the service rate from 50% to 83%. Carrier frequencies, carrier phases, and amplitudes are assumed to be perfectly estimated at the receiver. The amount of MAI is characterized by the signal to interference ratio SIR, i.e., the ratio between the power of the user of interest and the power of the interfering user. The performance of the MUD receivers is presented as a function of the SIR, the relative frequency shift $\Delta f/R$ where R is the symbol rate, and the E_b/N_0 ratio of the user of interest. The beacon signals are generated according to Section 2.1. Each simulation is based on the transmission of 80,000 symbols.

Figure 1 presents the BER performance of the MUD receivers. The ML detector achieves the best performance. The conventional receiver, the decorrelator, and the MMSE receiver are all inappropriate for the ARGOS system since they perform poorly when the signal of interest is corrupted by a a signal with a higher power. IC-based receivers perform better in these conditions. When SIR (dB) < 0, the interfering signal is decoded first, the SIC and the PIC receivers perform exactly the same computations (using the conventional receiver), and thus achieve the same BER performance. Inversely, when SIR (dB) > 0, the BER of the PIC receiver is higher than the one of the SIC receiver because the estimation of the interfering signal by the PIC receiver is not error-free so the IC is not performed well. The BER performance of the PIC receiver is improved when the conventional receiver is replaced by an MMSE receiver (MMSE-PIC receiver).

We now observe the E_b/N_0 ratio that is required in order to achieve a given BER [5]. In the single user case, the reference BER, denoted $BER^{\text{(ref)}} = 3.3 \times 10^{-3}$, is achieved at a reference E_b/N_0 ratio, $(E_b/N_0)^{\text{(ref)}} = 6.72$ dB. Let E_b/N_0 be the ratio that is required in order to achieve the BER performance $BER^{\text{(ref)}}$ in the multi-user case[§]. Hence, MUD receivers are evaluated according to the degradation factor δ defined as δ (dB) $= (E_b/N_0)$ (dB) $- (E_b/N_0)^{\text{(ref)}}$ (dB). Figure 2 presents degradation factors δ (dB) as a function of the SIR for different values of $\Delta f/R$. When the SIR is increasing and $SIR \gg 1$, the MAI decreases so the degradation factors are decreasing. Inversely, when the SIR is decreasing and $SIR \ll 1$, the interfering signal is successfully decoded so the IC performs well and the degradation factors converge toward the ones of the ML detector. The degradation factors decrease when $\Delta f/R$ is increasing because the correlation coefficients, and

---

[§]$BER^{\text{(ref)}}$ is the lowest observable BER, i.e., $1/304$, 304 being the maximal number of bits in an ARGOS message.

hence the MAI, depend on $\text{sinc}(\Delta f/R)$. The ML detector exhibits the best performance, followed by the MMSE-PIC, the PIC, and the SIC.

4. MUD RECEIVERS FOR ASYNCHRONOUS ARGOS USERS

We now consider the asynchronous case. The output of the matched filter is presented first. Then, MUD receivers are described.

4.1. Matched Filter Output and Matrix Representation

Let l be the user of interest, $l \in [1, K]$. The output of the matched filter for the uth symbol, $u \in [0, M]$, is defined as

$$y_l(u) = \int_{uT+\tau_l}^{(u+1)T+\tau_l} r(t) \exp[-j(2\pi\Delta f_l t + \theta_l')]h^*(t - uT - \tau_l)dt \tag{15}$$

where $\theta_l' = \theta_l - 2\pi\Delta f_l \tau_l$. By replacing the expression of $r(t)$ given by (3) in (15), the output $y_l(u)$ is written as

$$y_l(u) = \sum_{k=1}^{K} A_k \cos(m)\rho_{l,k}'(u) + j\sum_{k=1}^{K}\sum_{n=0}^{M-1} A_k \sin(m)b_k(m)\rho_{l,k}(u,n) + \eta_l(u) \tag{16}$$

where $\rho_{l,k}'(u)$ and $\rho_{l,k}(u,n)$ denote the time dependent cross correlation of the signature waveforms of user l and user k with $(l,k) \in [0, K]$, u denotes the received symbol for the user of interest l, and n denotes the received symbol for the interfering user k. The coefficients $\rho_{l,k}'(u)$ and $\rho_{l,k}(u,n)$ are given by

$$\rho_{l,k}'(u) = \int_{uT+\tau_l}^{(u+1)T+\tau_l} \exp\{j[2\pi(\Delta f_k - \Delta f_l)t + \theta_k' - \theta_l']\}h^*(t - uT - \tau_l)dt \tag{17}$$

$$\rho_{l,k}(u,n) = \int_{uT+\tau_l}^{(u+1)T+\tau_l} \exp\{j[2\pi(\Delta f_k - \Delta f_l)t + \theta_k' - \theta_l']\}h(t - nT - \tau_k)h^*(t - uT - \tau_l)dt \tag{18}$$

We note that the coefficients of (17) and (18) have also the Hermitian property. The noise component can be written as

$$\eta_l(u) = \int_{uT+\tau_l}^{(u+1)T+\tau_l} \exp[-j(2\pi\Delta f_l t + \theta_l')]h^*(t - uT - \tau_l)dt$$

We note that the symbol $b_l(u)$ of user l is correlated with the symbols $b_k(u)$ of the other $(K-1)$ users i.e., for $k \in [1, K]$ and $k \neq l$, with the symbols $b_k(u+1)$ of the preceding users i.e., for $k \in [1, l-1]$ and with the symbols $b_k(u-1)$ of the following users i.e., for $k \in [l+1, K]$ [17]. Thus, (16) is written as

$$
\begin{aligned}
y_l(u) &= \sum_{k=1}^{K} A_k \cos(m) \rho'_{l,k}(u) + j \sum_{k=1}^{K} A_k \sin(m) b_k(u) \rho_{l,k}(u, u) \\
&+ j \sum_{k=1}^{l-1} A_k \sin(m) b_k(u+1) \rho_{l,k}(u, u+1) + j \sum_{k=l+1}^{K} A_k \sin(m) b_k(u-1) \rho_{l,k}(u, u-1) \\
&+ \eta_l(u)
\end{aligned}
$$

The following computations of the correlation coefficients are based on both (17) and (18), and the $\zeta_{l,k}(a, b, u)$ functions given in (9). Recall that $h(t)$ is the unit energy signature waveform with a value of $1/\sqrt{T}$ over the interval $[0, T/2]$ and a value of $-1/\sqrt{T}$ over the interval $[T/2, T]$. In a similar way as in (8), the coefficients $\rho'_{l,k}(u)$ are given by

$$
\rho'_{l,k}(u) = \zeta_{l,k}(\tau_l, \tau_l + T/2, u) - \zeta_{l,k}(\tau_l + T/2, \tau_l + T, u) \tag{19}
$$

The computation of the coefficients $\rho_{l,k}(u, n)$ have been addressed in [17] for Non-Return-to-Zero (NRZ) signals. We present here the main results for a bi-phase signal. We begin with the case where $n = u - 1$. The coefficients $\rho_{l,k}(u, u-1)$ correspond to the correlation between the received symbol at instant $uT + \tau_l$ for the user of interest l and the received symbols at instant $(u-1)T + \tau_k$ of the interfering user k where $k \in [l+1, K]$. Thus, according to (4), we have $\tau_k > \tau_l$. So we have that

$$
\begin{aligned}
\rho_{l,k}(u, u-1) &= -\zeta_{l,k}(\tau_l, \tau_k, u) & \text{when } 0 < \tau_k - \tau_l \leq T/2 \\
\rho_{l,k}(u, u-1) &= \zeta_{l,k}(\tau_l, \tau_k - T/2, u) - \zeta_{l,k}(\tau_k - T/2, \tau_l + T/2, u) \\
&+ \zeta_{l,k}(\tau_l + T/2, \tau_k, u) & \text{when } T/2 < \tau_k - \tau_l < T
\end{aligned}
$$

In a similar way, we compute the coefficients $\rho_{l,k}(u, n)$ where $n = u + 1$. The coefficients $\rho_{l,k}(u, u+1)$ correspond to the correlation between the received symbol at instant $uT + \tau_l$ for the user of interest l and the received symbols at instant $(u+1)T + \tau_k$ of the interfering users k where

$k \in [1, l-1]$. Thus, using (4), we have $\tau_l > \tau_k$ and

$$
\begin{aligned}
\rho_{l,k}(u, u+1) &= -\zeta_{l,k}(\tau_k + T, \tau_l + T, u) &&\text{when } 0 < \tau_l - \tau_k \leq T/2 \\
\rho_{l,k}(u, u+1) &= \zeta_{l,k}(\tau_k + T, \tau_l + T/2, u) - \zeta_{l,k}(\tau_l + T/2, \tau_k + 3T/2, u) \\
&\quad + \zeta_{l,k}(\tau_k + 3T/2, \tau_l + T, u) &&\text{when } T/2 < \tau_l - \tau_k < T
\end{aligned}
$$

Finally, we compute the coefficients $\rho_{l,k}(u, n)$ where $n = u$. The coefficients $\rho_{l,k}(u, u)$ correspond to the correlation between the received symbol at instant $u + \tau_l$ for the user of interest l and the received symbols at instant $u + \tau_k$ of the interfering users k where $k \in [1, K]$ and $k \neq l$. We limit the computation to the case where $k \in [l, K]$, due to the Hermitian property of the coefficients. Thus, according to (4), we have $\tau_k \geq \tau_l$ and

$$
\begin{aligned}
\rho_{l,k}(u, u) &= \zeta_{l,k}(\tau_k, \tau_l + T/2, u) - \zeta_{l,k}(\tau_l + T/2, \tau_k + T/2, u) \\
&\quad + \zeta_{l,k}(\tau_k + T/2, \tau_l + T, u) &&\text{when } 0 \leq \tau_k - \tau_l < T/2 \\
\rho_{l,k}(u, u) &= -\zeta_{l,k}(\tau_k, \tau_l + T, u) &&\text{when } T/2 \leq \tau_k - \tau_l < T
\end{aligned}
$$

The matrix representation of $y_l(u)$ in the case of asynchronous transmissions is slightly different from the one in the synchronous case since additional terms must be taken into account

$$
\begin{aligned}
\mathbf{y}(u) &= \mathbf{R}'(u)\cos(m)\mathbf{A}\mathbf{1}_{K\times 1} + j\mathbf{R}(u, u)\sin(m)\mathbf{A}\mathbf{b}(u) + j\mathbf{R}(u, u-1)\sin(m)\mathbf{A}\mathbf{b}(u-1) \\
&\quad + j\mathbf{R}(u, u+1)\sin(m)\mathbf{A}\mathbf{b}(u+1) + \mathbf{n}(u)
\end{aligned}
$$

where $\mathbf{y}(u)$, $\mathbf{R}'(u)$, $\mathbf{R}(u, u)$, $\mathbf{A}$, $\mathbf{b}(u)$, $\mathbf{n}(u)$ are defined in Section 3, $\mathbf{R}(u, u-1) \in \mathbb{C}^{K \times K}$ is an upper triangular matrix with the (l, k) element equal to the cross correlation term $\rho_{l,k}(u, u-1)$ where $k \in [l+1, K]$, and $\mathbf{R}(u, u+1) \in \mathbb{C}^{K \times K}$ is a lower triangular matrix with the (l, k) element equal to the cross correlation term $\rho_{l,k}(u, u+1)$ where $k \in [1, l-1]$. We now complete the matrix representation of the $y_l(u)$ by taking into account all the indices u

$$
\mathbf{y} = \mathbf{R}'\cos(m)\mathbf{A}'\mathbf{1}_{KM\times 1} + j\mathbf{R}\sin(m)\mathbf{A}'\mathbf{b} + \mathbf{n} \tag{20}
$$

where we define $\mathbf{y} = [\mathbf{y}(0), \mathbf{y}(1), \ldots, \mathbf{y}(M-1)]^T$, $\mathbf{b} = [\mathbf{b}(0), \mathbf{b}(1), \ldots, \mathbf{b}(M-1)]^T$, and $\mathbf{n} = [\mathbf{n}(0), \mathbf{n}(1), \ldots, \mathbf{n}(M-1)]^T$. The matrices $\mathbf{A}'$ and $\mathbf{R}'$ are two $KM \times KM$ matrices defined as

follows

$$
\mathbf{A}' = \begin{pmatrix} \mathbf{A} & 0 & \dots & 0 \\ 0 & \mathbf{A} & \ddots & \vdots \\ \vdots & \ddots & \ddots & 0 \\ 0 & \dots & 0 & \mathbf{A} \end{pmatrix}, \quad \mathbf{R}' = \begin{pmatrix} \mathbf{R}'(0) & 0 & \dots & 0 \\ 0 & \mathbf{R}'(1) & \ddots & \vdots \\ \vdots & \ddots & \ddots & 0 \\ 0 & \dots & 0 & \mathbf{R}'(M-1) \end{pmatrix}
$$

Finally, the matrix $\mathbf{R}$ is a $KM \times KM$ matrix defined by

$$
\mathbf{R} = \begin{pmatrix} \mathbf{R}(0,0) & \mathbf{R}(0,1) & 0 & \dots & \dots & 0 \\ \mathbf{R}(1,0) & \mathbf{R}(1,1) & \mathbf{R}(1,2) & \ddots & \ddots & \vdots \\ 0 & \ddots & \ddots & \ddots & \ddots & \vdots \\ \vdots & \ddots & \mathbf{R}(u,u-1) & \mathbf{R}(u,u) & \mathbf{R}(u,u+1) & \vdots \\ \vdots & \ddots & \ddots & \ddots & \ddots & 0 \\ 0 & \dots & \dots & 0 & \mathbf{R}(M-1,M-2) & \mathbf{R}(M-1,M-1) \end{pmatrix}
$$

4.2. Multi-User Detection Techniques

According to the results of the previous section, only two MUD receivers are presented here: the ML detector and the SIC receiver. The MMSE-PIC is not considered since it involves the inversion of $KM \times KM$ matrices. This computational load makes this solution impractical.

4.2.1. Maximum Likelihood Detector
Following the same steps as in the previous section, we have that [18]

$$
\hat{\mathbf{b}} = \operatorname*{argmax}_{\mathbf{b} \in \mathbf{B}} \{ P[r(t), t \in [0, MT] | \mathbf{b}] \} = \operatorname*{argmax}_{\mathbf{b} \in \mathbf{B}} G[\mathbf{b}]
$$

where $\mathbf{B}$ is the set of all the possible sequences of the vector $\mathbf{b}$ and

$$
G[\mathbf{b}] = P[r(t), t \in [0, MT] | \mathbf{b}] = \frac{1}{\sqrt{2\pi\sigma^2}} \exp \left[\int_0^{MT} -\frac{1}{2\sigma^2} |r(t) - s_{\mathbf{b}}(t)|^2 dt \right] \tag{21}
$$

where $s_{\mathbf{b}}(t)$ is defined as

$$
s_{\mathbf{b}}(t) = \sum_{k=1}^{K} A_k [\cos(m) + j\sin(m) \sum_{n=0}^{M-1} b_k(n) h(t - nT - \tau_k)] \exp[j(2\pi \Delta f_k t + \theta'_k)]
$$

We rewrite (21) and suppress the terms that do not depend on $\mathbf{b}$. So, we have that

$$G[\mathbf{b}] = 2\,\mathrm{Re}\left(\int_0^{MT} r(t)s_{\mathbf{b}}^*(t)dt\right) - \int_0^{MT} s_{\mathbf{b}}(t)s_{\mathbf{b}}^*(t)dt = \Omega_1[\mathbf{b}] - \Omega_2[\mathbf{b}]$$

The first term $\Omega_1[\mathbf{b}]$ can be expressed as

$$\Omega_1[\mathbf{b}] = 2\,\mathrm{Re}\left(\sum_{k=0}^{K} A_k[\cos(m)r_k' - j\sum_{n=0}^{M-1}\sin(m)b_k(n)y_k(n)]\right)$$

where $r_k' = \int_0^{MT} r(t)\exp[j(2\pi\Delta f_k t + \theta_k')]dt$. The second term $\Omega_2[\mathbf{b}]$ can be written as

$$\begin{aligned}\Omega_2[\mathbf{b}] &= \sum_{k=1}^{K}\sum_{l=1}^{K} A_k A_l \left[\cos^2(m)\zeta_{l,k}(0,MT,0) + \sum_{n=0}^{M-1}\sum_{n'=0}^{M-1}\sin^2(m)b_k(n)b_l(n')\rho_{l,k}(n',n)\right] \\ &+ \Omega_3[\mathbf{b}]\end{aligned}$$

where $\Omega_3[\mathbf{b}] = -2\cos(m)\sin(m)\sum_{k=1}^{K}\sum_{l=1}^{K}\sum_{n=0}^{M-1} A_k A_l\,\mathrm{Im}[\rho_{l,k}'(n)]$. Using the hermitian property, we have that

$$\begin{aligned}G[\mathbf{b}] &= 2\,\mathrm{Im}\left[\sum_{k=1}^{K}\sum_{n}^{M-1} A_k \sin(m)b_k(n)y_k(n)\right] + \sum_{k=1}^{K}\sum_{l=1}^{K}\sum_{n=0}^{M-1}\sum_{n'=0}^{M-1} A_k A_l \sin^2(m)b_k(n)b_l(n')\rho_{l,k}(n',n) \\ &+ 2\,\mathrm{Im}\left[\sum_{k=1}^{K}\sum_{l=1}^{K}\sum_{n=0}^{M-1} A_k A_l \cos(m)\sin(m)b_k(n)\rho_{l,k}'(n)\right]\end{aligned}$$

The matrix form of the previous expression is given by

$$\begin{aligned}G[\mathbf{b}] &= 2\,\mathrm{Im}[\mathbf{b}^T(u)\sin(m)\mathbf{A}'\mathbf{y})] - \mathbf{b}^T(u)\sin^2(m)\mathbf{A}'\mathbf{R}\mathbf{A}'\mathbf{b} \\ &+ 2\,\mathrm{Im}[\mathbf{1}_{KM\times 1}^T\cos(m)\sin(m)\mathbf{A}'\mathbf{R}'\mathbf{A}'\mathbf{b}]\end{aligned}$$

Hence, the optimal detector consists of K matched filters followed by a detector based on an exhaustive search of the best symbol sequence in a set of 2^{KM} possible sequences. The computational load of this detector can be reduced using the Viterbi algorithm.

4.2.2. Successive Interference Cancellation (SIC) Receiver The design of a SIC receiver for asynchronous ARGOS users follows the same steps as in Section 3.2.5. The signal with the largest power is decoded first. This signal is regenerated based on the decoded symbols and the estimated version of the signal, $\hat{r}_{(1)}(t)$, is then subtracted to the received signal in order to demodulate the

signal with the second largest power. The signal with the second largest power is decoded by demodulating $r(t) - \hat{r}_{(1)}[t - \tau_{(1)}]$ where $\tau_{(1)}$ is the time delay of the user with the largest power. The method is repeated for subsequent users.

4.3. Simulations Results

We assume the reception of $K = 2$ users separated by a frequency shift Δf and a time delay $\Delta\tau$. The user of interest is received first. The performance of each MUD receiver is then presented as a function of $\Delta f/R$, $\Delta\tau/T$, the received E_b/N_0 ratio, and the SIR. Carrier frequencies, carrier phases, and amplitudes are assumed to be perfectly estimated at the receiver. Each simulation is based on the transmission of 80,000 symbols. Different relative frequency shifts give rise to different performance curves when the BER is plotted as a function of $\Delta\tau/T$ (see Figure 3). This is because the standard deviation of the MAI exhibits different shapes according to the values of $\Delta f/R$ (see Figure 4). Degradation factor curves are similar to BER curves (see Figure 5).

5. PERFORMANCE ANALYSIS

In the multi-user case, additional E_b/N_0 (dB) margins must be added to $(E_b/N_0)^{(\text{ref})}(\text{dB})$ in order to achieve a BER performance of $BER^{(\text{ref})}$. These margins depend on several parameters among which the frequency shifts and the time delays between the users. We now design an analysis tool in order to determine the range of values over which none, one, or more user signals can be successfully decoded. We focus here on SIC receivers since they achieve the best trade-off between BER performance and complexity. Moreover we restrict our study to the case $K = 2$. We define a decoding condition: user p is successfully decoded among a set of K users if its BER is less than or equal to $BER^{(\text{ref})}$, where $p \in [1, K]$. The three possible cases are: 0, 1, or 2 signals are successfully decoded. We study the occurrence of these three cases according to the value of the following parameters: the SIR, the received SNR per bit, the time difference $\Delta\tau$, and the frequency shift Δf between the two received signals. Furthermore, we assume perfect parameter estimation. The case of imperfect estimation is discussed later. We first define a loss factor for user p (see Figure 1 in [19])

$$\delta_p(\text{dB}) = (E_b/N_0)_p(\text{dB}) - (E_b/N_0)^{(\text{ref})}(\text{dB})$$

where $(E_b/N_0)_p$ is the SNR per bit that is needed to achieve a BER performance of $BER^{(\text{ref})}$ in a multi-user transmission for user p. Let $(E_b/N_0)_p^{(q)}$ be the SNR per bit that is needed on signal q to

achieve a successful decoding on user p. So we have that

$$
\begin{aligned}
\delta_p(\text{dB}) &= \delta_p^S(\text{dB}) + \delta_p^T(\text{dB}) \\
\delta_p^T(\text{dB}) &= (E_b/N_0)_p^{(q)}(\text{dB}) - (E_b/N_0)^{(\text{ref})}(\text{dB}) \\
\delta_p^S(\text{dB}) &= (E_b/N_0)_p(\text{dB}) - (E_b/N_0)_p^{(q)}(\text{dB})
\end{aligned}
\tag{22}
$$

Moreover we have that $\delta_p^S(\text{dB}) = SIR\,(\text{dB})$ if $p = 1$ and $q = 2$, and $\delta_p^S(\text{dB}) = -SIR\,(\text{dB})$ if $p = 2$ and $q = 1$. Similar definitions can be obtained for the degradation factors of user q. We define the performance indicator Δ_p as

$$
\Delta_p(\text{dB}) = \delta_q^T(\text{dB}) - \delta_p(\text{dB})
\tag{23}
$$

where $\delta_q^T(\text{dB})$ is obtained by replacing p by q in (22). So we have that

$$
(E_b/N_0)_p^{(q)}(\text{dB}) = (E_b/N_0)_p(\text{dB}) + \Delta_p(\text{dB})
$$

When user p achieves the BER target of $BER^{(\text{ref})}$ with an SNR per bit $(E_b/N_0)_p$, the performance indicator Δ_p (dB) depicts the margin that must be added to $(E_b/N_0)_p$ (dB) so that user q can achieve the same BER target of $BER^{(\text{ref})}$. So when the SNR per bit of user p is set to $(E_b/N_0)_p$ (dB) and Δ_p (dB) > 0, this means that user p is successfully decoded but also that the SNR per bit on user p should be higher in order to successfully decode user q, so only one user is decoded in this case (user p). The other results are gathered in Table I). The BER curves of both user p and q are used for the computation of Δ_p (dB). From the BER curve of user q, we get δ_q. From (22) and δ_q^S—that equals SIR or $1/SIR$—, we get δ_q^T. Then, from the BER curve of user p, we get δ_p and hence Δ_p is determined through (23).

Figure 6 has been obtained with a BER target of $BER^{(\text{ref})} = 3.3 \times 10^{-3}$, $K = 2$, $p = 1$, and $q = 2$. We have that Δ_p (dB) is negative for all $\Delta\tau/T$, so both signals are successfully decoded when user p is successfully decoded. The maximum degradation factor is 6.9 dB, so user p is successfully decoded when $(E_b/N_0)_p$ (dB) is higher than 13.62 dB, taking into account the reference SNR per bit $(E_b/N_0)^{(\text{ref})}$ of 6.72 dB. Moreover, the minimum $(E_b/N_0)_q$ (dB) that is needed to allow a successful decoding of user q is 16.62 dB since the SIR (dB) is 3 dB. Note that when the SNR per bit of user p is 10 dB, i.e., when the SNR per bit of user p is 3.28 dB above $(E_b/N_0)^{(\text{ref})}$, user p is successfully decoded for delays in the intervals $[0.00793T, 0.455T]$ and $[0.5793T, 0.955T]$, i.e., in 75% of the cases. Similar figures can be obtained for different values of $\Delta f/R$. Figure 7 summarizes all these

results for a $(E_b/N_0)_p$ (dB) of 10 dB. This figure is useful since it points out the range of values over which the system is operational.

Similar figures have been obtained for different values of $\Delta\tau$, Δf, and $(E_b/N_0)_p$. For symmetry reasons, the relative delays $\Delta\tau/T$ and the relative frequency shifts $\Delta f/R$ have been assumed to be uniformly distributed over $[0, 1]$ and $[0, 4]$, respectively¶. Moreover, experimental results have shown that the received $(E_b/N_0)_p$ (dB) could be approximated by a Gaussian law with mean 25.5 dB and standard deviation 4.83 dB. In a last experiment, we have randomly generated 7,000 values for the E_b/N_0 (dB) ratio (actually two values for each draw), 40 values for the relative frequency shift $\Delta f/R$, and 10 values for the relative delay $\Delta\tau/T$. With the previous results at hand, we have observed that the $K = 2$ users could be successfully decoded in 98% of the 2,800,000 cases. With a population of 37,600 beacons, the maximum service rate would be 84.6% if the MUD receiver could operate in 100% of the cases. With 98%, the achieved service rate is 83%.

We now address the issue of imperfect parameter estimation. Parameter estimation for multi-user communications systems have been already proposed in [18–26]. Additional E_b/N_0 (dB) margins must be added to the received SNR per bit in order to achieved the reference BER performance $BER^{(\text{ref})}$. Simulation results have shown that the percentage of successful decoding decreases to 80% of the 2,800,000 cases. So the service rate is now 67%. This service rate is still high compared to the estimated 50% service rate that could achieve a single-user receiver in the same conditions. This completes the validation step of our proposal.

6. CONCLUSION

The service rate of the ARGOS satellite system is decreasing with the increasing number of beacons. MUD receivers have been proposed to tackle this issue. In the synchronous case, typical linear receivers - conventional receiver, decorrelator, and MMSE receiver- are unable to successfully decode two beacon signals that arrive simultaneously at the satellite when the power of the interfering signal is higher than the power of the signal of interest. In this context, the ML detector and IC based receivers—SIC and PIC—provide the best performance in terms of BER. In the asynchronous case, preliminary computations show that only SIC receivers could be practically implemented. The performance of SIC receivers have been evaluated and compared to the performance of the ML detector. Simulation results also highlight the degradation factors of

---

¶The frequency shifts are limited to $[0, 4R]$ since the power of a bi-phase signal is concentrated in the $[-4R, 4R]$ band.

the E_b/N_0 ratio required to achieve the reference BER performance of 3.3×10^{-3}. The analysis of these degradation curves shows that SIC receivers can successfully handle 98% of the transmission conditions. When imperfect estimates of the signal parameters are considered, the percentage falls to 80%, so the achieved service rate is 67% when the number of beacons is set to 37,600. This result is still acceptable compared to the service rate provided by single user receivers, i.e., 50%. Note that this service rate of 67% is a lower bound since it has been assumed that it is not possible to decode beacon signals when three or more signals arrive at the same time at the satellite. This is a worst case scenario. Simulations involving at least three users should be done in order to evaluate the practical service rate. This could possibly provide a more realistic estimation for the performance of our proposed MUD receivers. This is left for future work.

REFERENCES

1. "ARGOS: Worldwide Tracking and Environmental Monitoring by Satellite," http://www.argos-system.org.

2. D. Clark, "Overview Of the Argos System," in *Proceedings of OCEANS'89*, 1989, pp. 934–939.

3. CNES, "Platform Transmitter Terminal (PTT-A2) Platform Message Transceiver (PMT-A2) - Physical Layer System Requirements," in *AS3-SP-516-274-CNES*, 2006.

4. S. Verdú, "Multiuser Detection." Cambridge Press, 1998.

5. R. Lupas and S. Verdú, "Linear Multiuser Detectors for Synchronous Code-Division Multiple-Access Channels," *IEEE Transactions on Information Theory*, vol. 35, no. 1, pp. 123–136, 1989.

6. E. Biglieri, G. Caire, J. E. Hakegaard, G. Taricco, and J. Ventura-Traveset, "System capacity enhancement by using multi-user processing techniques in narrowband satellite mobile communications," in *Fifth International Conference on Satellite Systems for Mobile Communications and Navigation*, 1996.

7. R. De Gaudenzi, T. Garde, F. Giannetti, and M. Luise, "DS-CDMA techniques for mobile and personal satellite communications: An overview," in *IEEE Second Symposium on Communications and Vehicular Technology in the Benelux*, 1994.

8. M. Zhou, A.-J. van der Veen, and R. van Leuken, "Multi-user leo-satellite receiver for robust space detection of ais messages," in *ICASSP*, 2012, pp. 2529–2532.

9. M. Picard, M. R. Oularbi, G. Flandin, and S. Houcke, "An Adaptive Multi-User Multi-Antenna Receiver for Satellite-Based AIS Detection," in *6th Advanced Satellite Multimedia Systems Conference and the 12th Signal Processing for Space Communications Workshop*, 2012.

10. M. M. Shihabi, T. M. Nguyen, and S. M. Hinedi, "A comparison of telemetry signals in the presence and absence of a subcarrier," *IEEE Transactions on Electromagnetic Compatibility*, vol. 36, no. 1, pp. 60–73, 1994.

11. F. Fares, M.-L. Boucheret, B. Escrig, T. Calmettes, and H. Guillon, "Multiuser Detection for Time Synchronous ARGOS Signals," in *Proc. International Communications Satellite Systems Conference (ICSSC)*, 2009.

12. J. M. Holtzman, "Successive Interference Cancellation for Direct Sequence Code Division Multiple Access," in *Proceedings of MILCOM*, 1994, pp. 997–1001.

13. P. Patel and J. Holtzman, "Analysis of a Simple Successive Interference Cancellation Scheme in a DS/CDMA System," *IEEE Journal on Selected Areas in Communications*, pp. 796–807, 1994.

14. D. Divsalar, M. K. Simon, and D. Raphaeli, "Improved Parallel Interference Cancellation for CDMA," *IEEE Transactions on Communications*, pp. 258–268, 1998.

15. H. Arslan and K. Molnar, "Cochannel Interference Suppression with Successive Cancellation in Narrow-Band Systems," *IEEE Communications Letters*, vol. 5, no. 2, pp. 37–39, 2001.

16. M. Moretti, G. J. M. Janssen, and R. Prasad, "Performance Evaluation of the Dual Signal Receiver for a Quadrature Modulation Scheme," in *Proceedings of the IEEE Global Telecommunications Conference (GLOBECOM)*, 1998, pp. 3542–3547.

17. F. Fares, M.-L. Boucheret, B. Escrig, T. Calmettes, and H. Guillon, "Multiuser Detection for Time Asynchronous ARGOS Signals," in *Proc. IEEE, IET International Symposium on Communication Systems, Networks and Digital signal Processing (CSNDSP)*, 2010.

18. S. Verdú, "Minimum Probability of Error for Asynchronous Gaussian Multiple-Access Channels," *IEEE Transactions on Information Theory*, vol. 32, pp. 85–96, 1986.

19. B. Escrig, F. Fares, M.-L. Boucheret, T. Calmettes, and H. Guillon, "Impact of Imperfect Parameter Estimation on the Performance of Multi-User ARGOS Receivers," in *IEEE Global Telecommunications Conference (GLOBECOM)*, 2010.

20. A. J. Viterbi and A. M. Viterbi, "Nonlinear Estimation of PSK-Modulated Carrier Phase with Applications to Burst Digital Transmission," *IEEE Transactions on Information Theory*, vol. 29, pp. 543–551, 1983.

21. G. De Jonghe and M. Moeneclaey, "The effect of the averaging filter on the cycle slipping of NDA feedforward carrier synchronizers for MPSK," in *Proc. IEEE International Conference on Communications (ICC)*, 1992.

22. X. Zhenhua, K. Rushforth, T. Short, and K. Moon, "Joint Signal Detection and Parameter Estimation in Multiuser Communications," *IEEE Transactions on Communications*, vol. 41, no. 7, pp. 1208–1216, 1993.

23. K. Moon and X. Zhenhua, "Parameter Estimation in a Multi User Communication System," *IEEE Transactions on Communications*, vol. 42, no. 8, pp. 2553–2560, 1994.

24. G. D. Jonghe and M. Moeneclaey, "Optimal Averaging Filter Length of the Viterbi & Viterbi Carrier Synchronizer for a Given Frequency Offset," in *Proc. IEEE Global Telecommunications Conference (GLOBECOM)*, 1994.

25. F. Daffara and J. Lamour, "Comparison Between Digital Phase Recovery Techniques in the Presence of a Frequency Shift," in *Proc. IEEE International Conference on Communications (ICC)*, 1994, pp. 940–945.

26. G. Janssen and S. Ben Slimane, "Symbol Error Probability Analysis of a Multiuser Detector for M-PSK Signals based on Successive Cancellation," *IEEE Journal on Selected Areas in Communications*, vol. 20, no. 2, pp. 330–338, 2002.

Table I. Successfully Decoded Users as a Function of the Performance Indicator

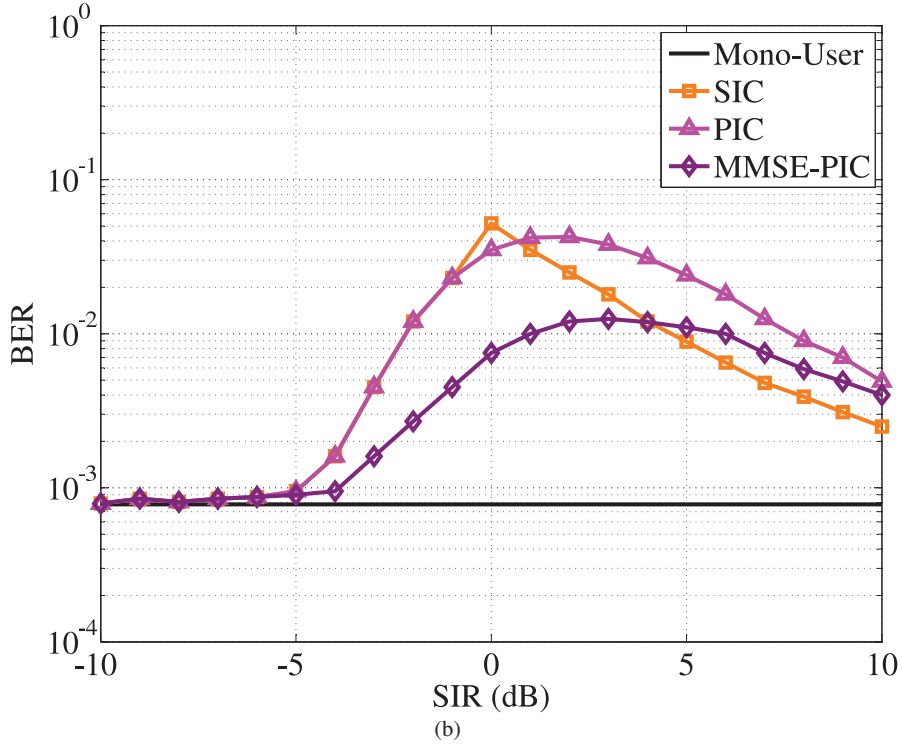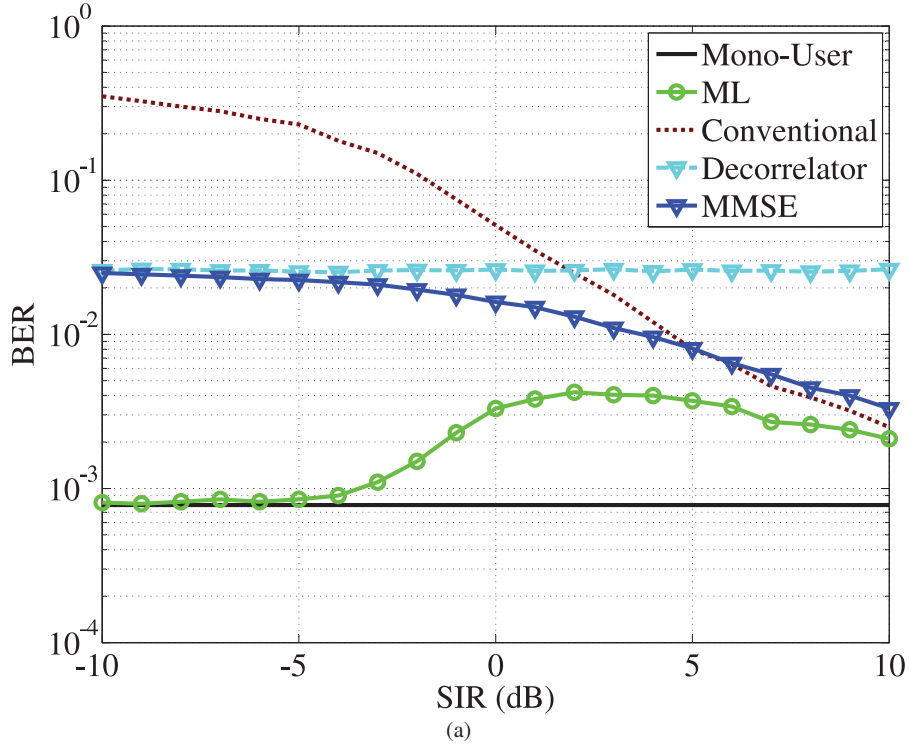|	$(E_b/N_0)_p \geq (E_b/N_0)^{\text{(ref)}}$	$(E_b/N_0)_q \geq (E_b/N_0)^{\text{(ref)}}$
$\Delta_p(\text{dB}) > 0$	p	p and q
$\Delta_p(\text{dB}) < 0$	p and q	q

Figure 1. BER curves of MUD receivers for synchronous ARGOS users as a function of the SIR in dB, $E_b/N_0 = 8$ dB and $\Delta f/R = 0.375$. (a) Four MUD receivers (ML Detector, Conventional Receiver, Decorrelator, and MMSE Receiver) are compared to the mono-user detector. (b) Three MUD receivers based on an IC approach (SIC, PIC, and MMSE-PIC) are compared to the mono-user detector.
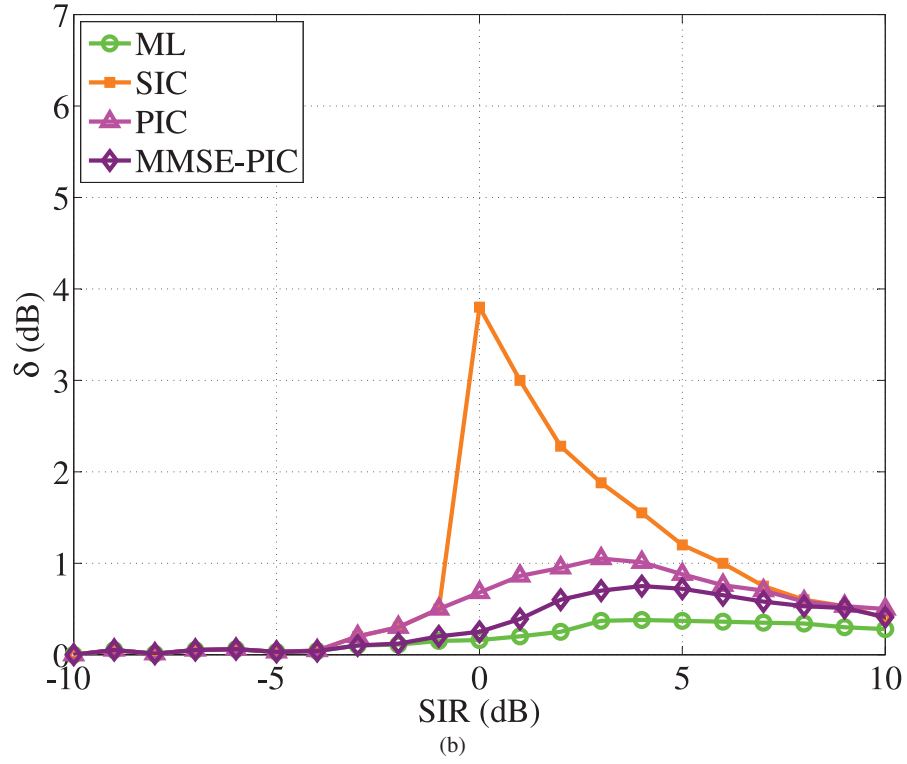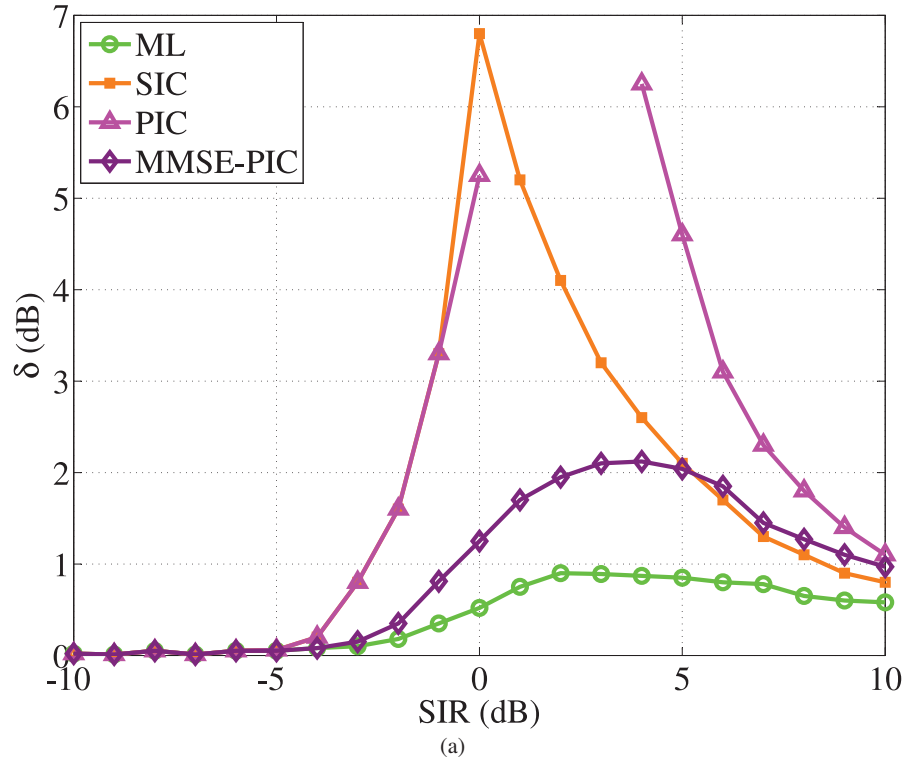
Figure 2. Degradation factors δ (dB) for $BER^{(\text{ref})} = 3.3 \times 10^{-3}$ as a function of the SIR in dB for $\Delta f / R = 0.475$ (a) and $\Delta f / R = 0.6$ (b). Four receivers are compared: the ML detector and three IC receivers (SIC, PIC, and MMSE-PIC).
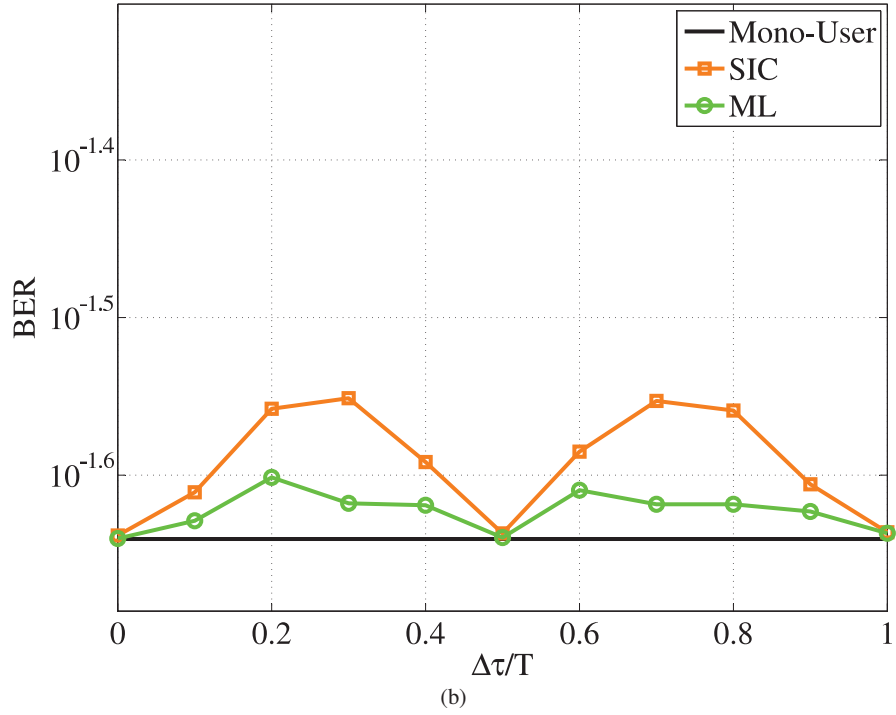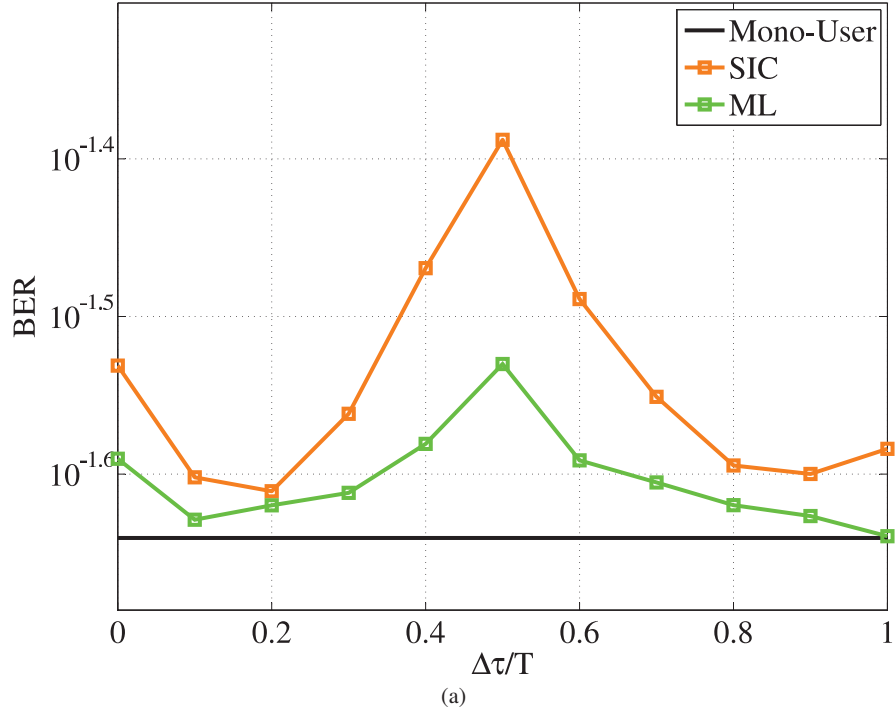
Figure 3. BER curves of MUD receivers for asynchronous ARGOS users as a function of the relative delay difference $\Delta\tau/T$, for $SIR = 3$ dB, $E_b/N_0 = 8$ dB, $\Delta f/R = 0.75$ (a) and $\Delta f/R = 1$ (b). Two MUD receivers (ML Detector and SIC receiver) are compared to the mono-user receiver.
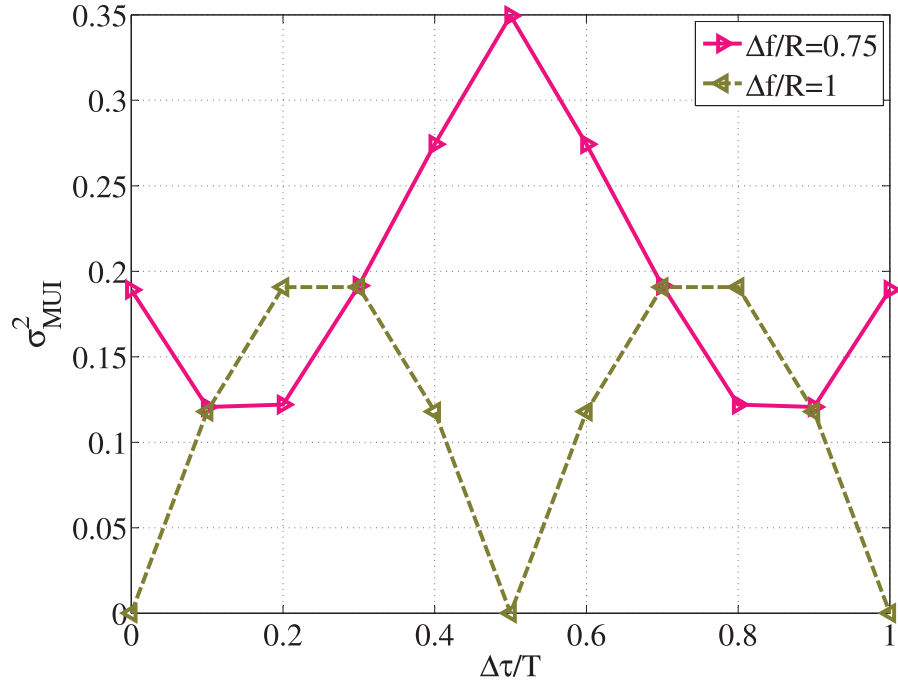
Figure 4. Variance of the MUI as a function of the relative delay difference $\Delta\tau/T$, for $\Delta f/R = 0.75$ and $\Delta f/R = 1$.
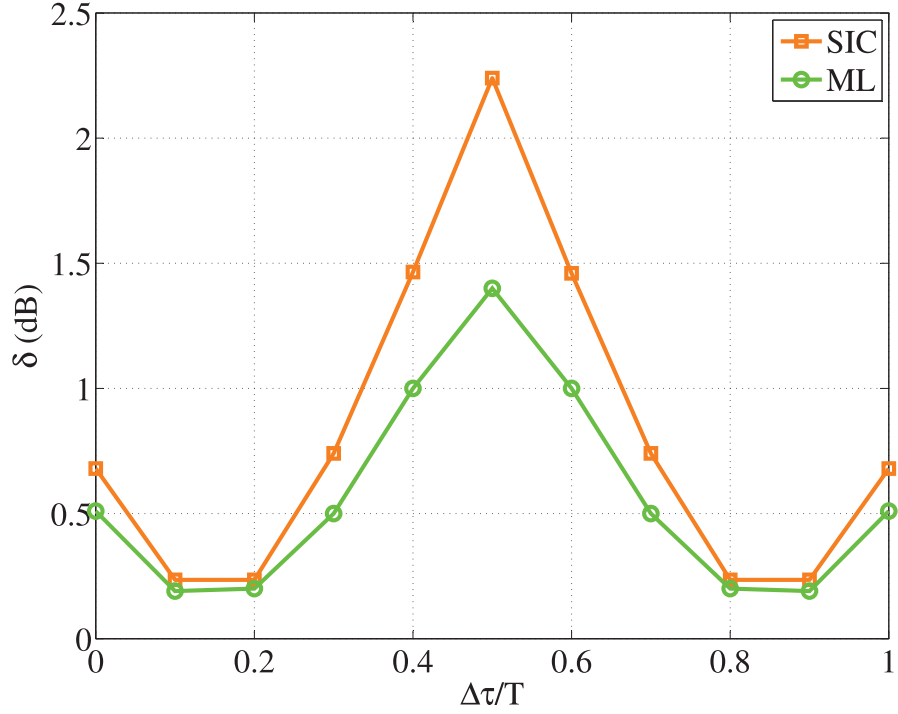

Figure 5. Degradation factors δ (dB) for $BER^{(\text{ref})} = 3.3 \times 10^{-3}$ as a function of the relative delay difference $\Delta\tau/T$, for $\Delta f/R = 0.75$ and $SIR = 3$ dB. Two MUD receivers (ML Detector and SIC receiver) are compared.
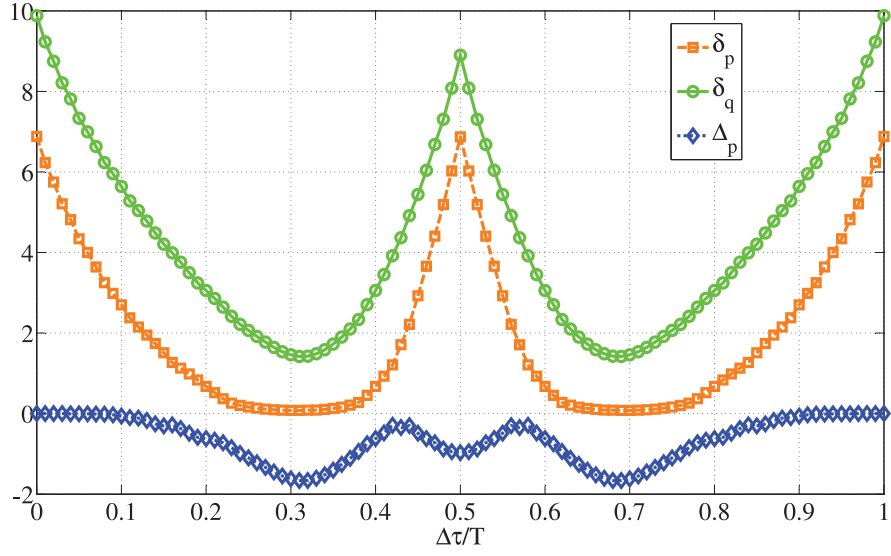
Figure 6. Degradation factors δ_p(dB), δ_q(dB), and Δ_p(dB) for $BER^{(\text{ref})} = 3.3 \times 10^{-3}$ as a function of the relative delay difference $\Delta\tau/T$, for $\Delta f/R = 0$ and $SIR = 3$ dB.
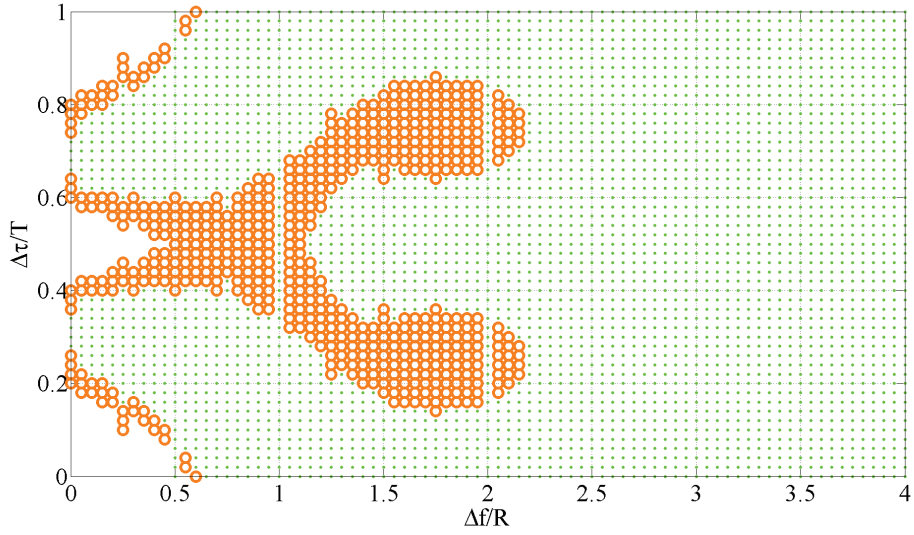

Figure 7. Area of successful decoding as a function of the relative frequency shift $\Delta f/R = 0$ and the relative time delay $\Delta\tau/T$, for $SIR = 10$ dB and a received SNR per bit δ_p(dB) of 10 dB. The dots denote the cases for which both users are successfully decoded. The circles denote the cases for which only one user is decoded, and there is no marker when none of the two users has been decoded.